A design method of broadband metalens using time-domain topology optimization

H. Yasuda and S. Nishiwaki

View Online   Export Citation   CrossMark

ARTICLES YOU MAY BE INTERESTED IN

Computational inverse design for ultra-compact single-piece metalenses free of chromatic and angular aberration
Applied Physics Letters **118**, 041104 (2021); https://doi.org/10.1063/5.0035419

CMOS-compatible all-dielectric metalens for improving pixel photodetector arrays
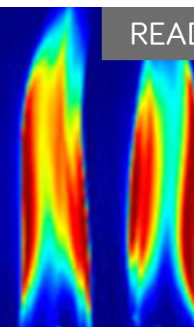APL Photonics **5**, 116105 (2020); https://doi.org/10.1063/5.0022162

A reconfigurable active acoustic metalens
Applied Physics Letters **118**, 133502 (2021); https://doi.org/10.1063/5.0045024

AIP Advances
Fluids and Plasmas Collection

READ NOW

A design method of broadband metalens using time-domain topology optimization

View Online   Export Citation   CrossMark

H. Yasuda[a] (ID) **and S. Nishiwaki**

AFFILIATIONS

Department of Mechanical Engineering and Science, Kyoto University, Kyotodaigaku-Katsura, Kyoto 615-8540, Japan

[a] Author to whom correspondence should be addressed: yasuda.hideki.23x@st.kyoto-u.ac.jp

ABSTRACT

Flat metalenses have attracted attention due to an increasing demand for compact electromagnetic devices. For such applications, broadband metalenses are highly desirable; however, conventional metalenses show relatively narrow band operation. Here, we propose a design method of free-form metalenses using topology optimization to operate with enhanced bandwidths. In contrast with preceding reports of topology optimization methods for metalenses, we developed a topology optimization method based on the time domain formulation to deal with broadband frequencies simultaneously. For this purpose, a group delay of optical pulses in the time domain, which is equivalent to the broadband phase matching condition in the frequency domain, is employed in the objective function. A level set based topology optimization method is applied to obtain a clear optimal configuration. To demonstrate the effectiveness of the proposed method, we provide design examples of metalens unit cells at millimeter frequency. We confirm that optimized unit cells of metalenses show superior performance compared to the conventional unit cells for both transmittance efficiency and phase error in broadband wavelength.

I. INTRODUCTION

Electromagnetic metamaterials are engineered materials that have extraordinary optical properties that cannot be found in nature.[1] Such properties can be potentially applied for the development of novel optical devices, such as super-resolution microscopy and optical cloaking. Recently, two-dimensional flat metasurfaces have attracted much attention.[2–5] Among them, metalenses have attracted intense interest due to their wide range of industrial applications, such as cameras, virtual/augmented reality devices, microscopy, and lithography.[6–9] However, reported metalenses have shown relatively narrow band operation because of the chromatic dispersion produced by a diffraction of periodic cells and resonant light confinement in a unit cell structure. Although employing multiple coupled resonances[10,11] or stacking multiple layers of metasurfaces[12] has been proposed for broadening the operation bandwidth, the proposed metalenses have shown relatively narrow band operation.

Conventionally, the design approach of a metalens unit cell starts with the choice of a simple resonant structure, such as cylinders and rectangles. Then, the transmittance phase retardation of the unit cell is calculated for various geometrical parameters, such as radius, width, and depth. However, the number of degrees of parameters in these simple structures is limited, which makes it difficult to optimize metalenses for working in broadband wavelength.

The topology optimization method and inverse design method have been recently proposed as design methods of metalenses.[13–15] Free-formed metalenses designed by these methods attain improved performance and enhanced functionalities. In the millimeter wave frequency, where metalens structures are relatively huge, inverse designed metalenses have been already fabricated by using additive manufacturing. Although the development of innovative fabrication technology would be required, topology optimization design methods will be eventually applied in the optical domain, where strong demand for use in industrial applications exists.

So far, the proposed topology optimization methods of metalenses have been formulated as frequency domain methods. To consider the problem of designing a metalens for broadband operation in the frequency domain, a multi-objective formulation by selecting a set of frequencies is necessary. In order to solve such design problems, the electromagnetic field should be evaluated for all selected frequencies and hence will increase the computation time.

Recently, we proposed a level set based time-domain topology optimization method for the design of nanophotonic structures to control the spatiotemporal profile of optical pulses.[16] One advantage of time-domain analysis is that a band of frequencies can be effectively treated simultaneously, which is suitable for broadband optimization problems.

In this paper, we extend our previous research for the design of broadband metalenses. To achieve this, we defined the objective function using a group delay of optical pulses in the time domain, which is equivalent to the broadband phase matching condition for metalenses in the frequency domain. A level set based topology optimization method is applied to obtain an optimal configuration. To confirm the effectiveness of the proposed method, we provide design examples of metalens unit cells at millimeter frequency. We also present simple shape optimization design with constraint.

II. DESIGN METHOD OF METALENS

First, we briefly explain the concept of broadband topology optimization of metalenses using time domain formulation. Consider a metalens shown in Fig. 1. The metalens is composed of microstructures fabricated on the flat substrate, which provide the position dependent transmittance phase retardation for focusing. For broadband operation, the relative phase retardation $\varphi(r, \omega)$, which depends on the radial coordinate r and the angular frequency ω, provided by the metalens unit cells with respect to the center follows

$$\varphi(r, \omega) = -\frac{\omega}{c}\left(\sqrt{r^2 + F^2} - F\right), \tag{1}$$

where c and F are the speed of light and focal length of the metalens, respectively.

In the frequency domain, the objective function of the metalens design problem for broadband operation can be simply defined using the target electromagnetic field $E_T(r, \omega)$ as follows:

$$F(r) = \int_{-\infty}^{\infty} |E(r, \omega) - E_T(r, \omega)|^2 d\omega, \tag{2}$$

$$E_T(r, \omega) = \sqrt{\frac{n_2}{n_1}} e^{-i\frac{\omega}{c}\left(\sqrt{r^2 + F^2} - F\right)} E_{input}(r, \omega), \tag{3}$$

where $E(r, \omega)$ is the transmitted electromagnetic field, $E_{input}(r, \omega)$ is the input electric field, n_1 is the refractive index of the air, and n_2 is the refractive index of the substrate. The factor of n_2/n_1 denotes the wave-impedance ratio between the air and the substrate.

There are several problems to naively employ Eq. (2) for the design problem of broadband metalenses. First, several appropriate frequencies must be selected before the design, and a multi-objective formulation dealing with selected frequencies is required. However, determining the appropriate number of frequencies and selecting appropriate frequencies are difficult, and such choices are critical if high-performance metalenses are to be obtained. Second, a calculation is required for every selected wavelength, which typically results in a huge increase in the computation time.

Alternatively, we propose to conduct the optimization process using the time domain electromagnetic field. Using Parseval's theorem of the Fourier transform, Eq. (2) can be rewritten as follows:

$$\tilde{F}(r) = 2\pi \int_{-\infty}^{\infty} |\tilde{E}(r, t) - \tilde{E}_T(r, t)|^2 dt, \tag{4}$$

where $\tilde{E}(r, t)$ is the Fourier transforms of $E(r, \omega)$. $\tilde{E}_T(r, t)$ is the Fourier transforms of $E_T(r, \omega)$ and can be expressed as follows:

$$\tilde{E}_T(r, t) = \sqrt{\frac{n_2}{n_1}} \tilde{E}_{input}(r, t - \delta t(r)), \tag{5}$$

$$\delta t(r) = \frac{\sqrt{r^2 + F^2} - F}{c}, \tag{6}$$

where $\tilde{E}_{input}(r, t)$ is the Fourier transforms of $E_{input}(r, \omega)$.

The physical meaning of Eq. (5) is that the phase matching condition in the frequency domain can be transformed into the group delay $\delta t(r)$ of the input pulse in the time domain.[10] This is schematically shown in Fig. 1(b), where the metalens provides spatially dependent group delays such that optical pulses from different locations arrive simultaneously at the focus.
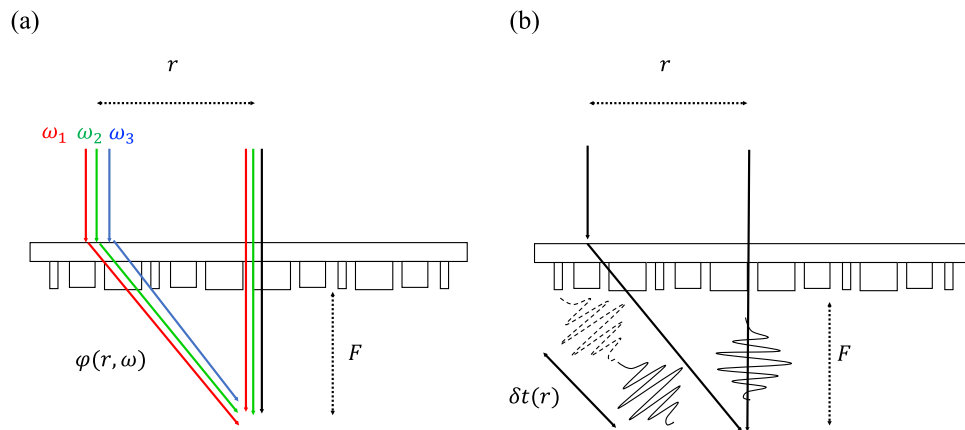
(a)   (b)

FIG. 1. A schematic illustration of the operation of the metalens: (a) in the frequency domain and (b) in the time domain.

One advantage to the use of the time domain calculation is that it is not necessary to select appropriate frequencies for defining the multi-objective function. Another advantage is the shorter computation time because $\tilde{E}(r, t)$ can be calculated in the single time domain calculation.

Next, we describe the topology optimization method. In this research, we employ the level set based topology optimization method proposed by Yamada et al.[17] In this method, structural boundaries are represented by the iso-surface of a scalar function, and clear and smooth optimal configurations can be obtained. Level set based topology optimization methods have been applied to a range of nanophotonic design problems, such as metamaterials with negative permittivity, light-trapping, and optical cloaking structures.[18–20]

In the proposed method, the relative electric permittivity ε is described using the characteristic function $X(\phi)$ as follows:

$$\varepsilon(\chi) = \varepsilon_0 + (\varepsilon_1 - \varepsilon_0)\chi(\phi). \tag{7}$$

Here, it is assumed that the dielectric metalens with permittivity ε_1 is embedded in a homogeneous medium with permittivity ε_0.

The characteristic function $X(\phi)$ is then introduced,

$$\begin{cases} \chi(\phi) = 1 & if \quad \phi \geq 0, \\ \chi(\phi) = 0 & if \quad \phi < 0, \end{cases} \tag{8}$$

where ϕ is the level set function defined as

$$\begin{cases} 0 < \phi(x) \leq 1 & if \quad \forall x \in \Omega \backslash \partial\Omega, \\ \phi(x) = 0 & if \quad \forall x \in \partial\Omega, \\ -1 \leq \phi(x) \leq 0 & if \quad \forall x \in D \backslash \Omega, \end{cases} \tag{9}$$

where D is a fixed design domain and Ω is a domain with permittivity ε_1. The level set function ϕ is used to represent the boundaries of the dielectric material, where positive values represent the material domains, negative values represent the surrounding medium domains, and zero represents the structural boundaries.

In the proposed topology optimization approaches, the level set function is evolved using the following equation during the optimization process by introducing friction time t':

$$\frac{\partial\phi}{\partial t'} = -K\left(\frac{\delta\tilde{F}}{\delta\chi} - \tau\nabla^2\phi\right), \tag{10}$$

where K is the proportionality coefficient and τ is a regularization parameter that adjusts the degree of regularization. Functional derivative $\delta\tilde{F}/\delta\chi$ can be derived as follows using the adjoint variable method:[21,22]

$$\frac{\delta\tilde{F}}{\delta\chi} = -(\varepsilon_1 - \varepsilon_0)\int_0^\infty \left[\lambda \cdot \left(\frac{\partial\tilde{E}}{\partial t}\right)\right]dt, \tag{11}$$

where λ is the adjoint vector.

In the above topology optimization method, any topological changes are allowed. In this study, we also included the shape optimization design in order to obtain a simple and manufacturable shape by imposing a constraint, in which only the vertical movement of the upper exterior cells is allowed. Under this constraint, the generation of interior cavities during the optimization process is prohibited. A similar constraint was employed for the design of a microlens array.[23] In the following, we call the optimization method with constraint as "shape optimization," and the optimization method without constraint as "topology optimization."

III. DESIGN EXAMPLE OF METALENS

Here, we provide design examples of metalens unit cells at millimeter frequency (78 GHz) to confirm the effectiveness of the proposed shape and topology optimization methods. We consider the design problem of unit cells of metalens, which provide specific group delays in the time domain. For simplicity, we limit the discussion to a 2D electromagnetic wave problem, but the presented algorithm can be easily extended to 3D metalens design. To obtain the time domain electric field $\tilde{E}(r, t)$, we employed the Finite-Difference Time-Domain (FDTD) method, which is one of the most popular methods for analyzing the properties of metalenses.

The 2D analysis model is shown in Fig. 2. The computational domain is divided into 80×300 square cells, and the size of each cell is 35 μm. Note that the period of the metalens unit cells is smaller than the wavelength of the center frequency and diffractions do not occur. The fixed design domain with 80×120 cells is located on the substrate whose permittivity is $\varepsilon_2 = 2.25$. An observation plane of transmitted pulse is located 175 μm below the fixed design domain. In this study, we chose the average value of Eq. (4) across the observation surface as the objective functional for the design of the unit cells. The solid material has a high effective permittivity $\varepsilon_1 = 4.0$, and the void material is air with an effective permittivity of $\varepsilon_0 = 1.0$. The incident waves $\tilde{E}_{input}(r, t)$ propagate from top to bottom and are
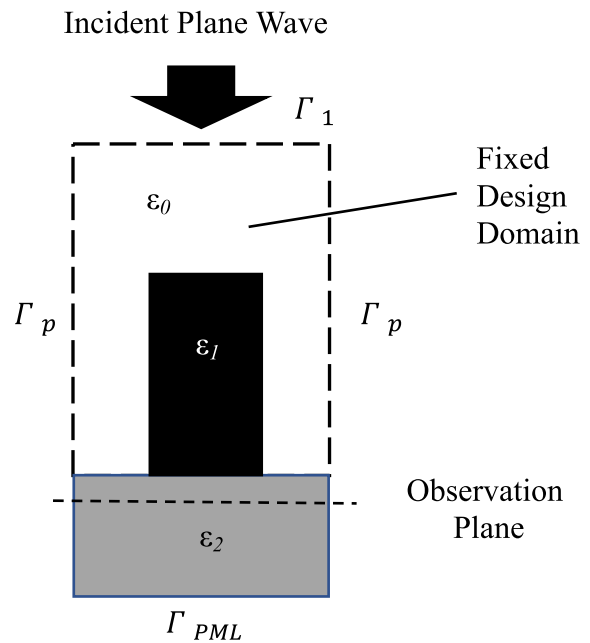

FIG. 2. A schematic of the analysis model.

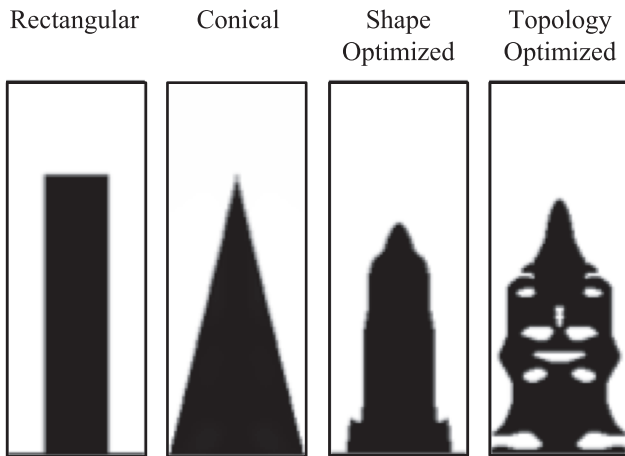Rectangular   Conical   Shape Optimized   Topology Optimized

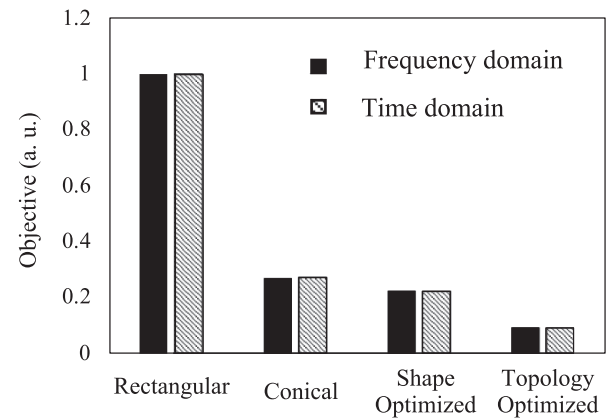**FIG. 3.** Designed unit cells.

FIG. 4. Objective function values of rectangular, conical, shape optimized, and topology optimized unit cells.

assumed to be TM plane waves with a center frequency of 78 GHz in the form of a Gaussian pulse modulated by sinusoidal waves.

To provide plane wave illumination, a total-field/scattered-field (TF/SF) virtual surface is adopted for a boundary Γ_1. A perfectly matched layer boundary condition and periodic boundary conditions are adopted for boundaries Γ_{PML} and Γ_P, respectively.

As an example, a metalens unit cell, which provides 9.6 ps group delay in the time domain, was considered. This group delay is equivalent to the transmittance phase retardation of $\varphi = 1.5\pi$ rad for a 78 GHz wave in the frequency domain.

Figure 3 shows the shape optimized and topology optimized structures, accompanied with a rectangular unit cell and a conical unit cell, which are employed in conventional metalens design. Note that the rectangular unit cell has 5.78 mm height and 1.4 mm width, whose volume approximately provides $\varphi = 1.5\pi$ rad transmittance phase retardation for a 78 GHz wave. The shape optimized

structure is similar to the conical structure, but it attains surface modification. The topology optimized structure is more complicated with void structures in the interior. These surface modification and inner voids correct the phase mismatch and improve the performance of the metalens, as we show later. In both cases, the material interfaces are clear and no grayscale regions appear in the optimal structure.

The obtained values of the objective function in the frequency domain [Eq. (2)] and time domain [Eq. (4)] are shown in Fig. 4. The values of objective function are drastically reduced for the shape and topology optimized cells compared with that of the rectangular unit cell. In addition, the value of objective function in the frequency domain is exactly the same as that in the time domain. This shows the justification of our proposal to use time domain formulation instead of frequency domain formulation for the broadband metalens optimization.
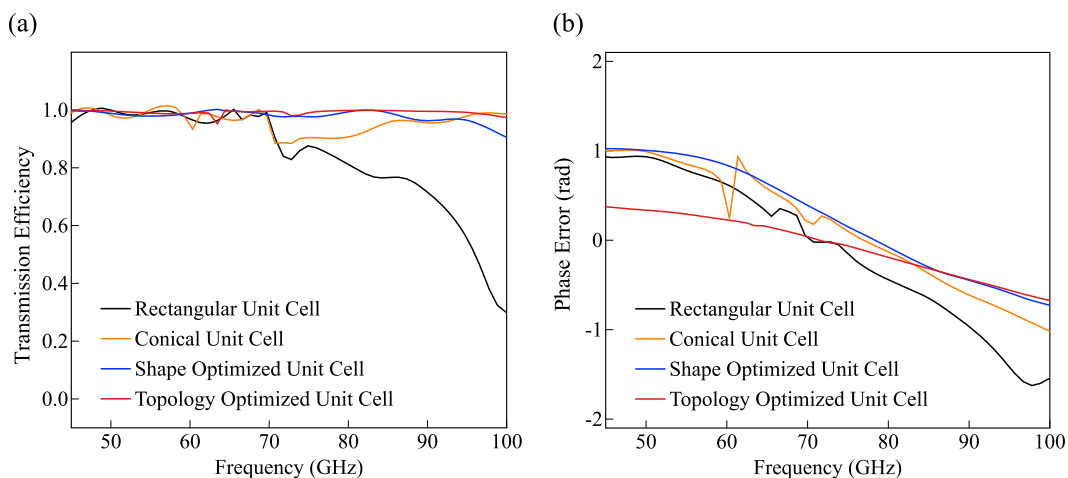
(a)   (b)

FIG. 5. Transmittance efficiencies and phase errors of rectangular, conical, shape optimized, and topology optimized unit cells: (a) transmittance efficiencies and (b) phase errors.
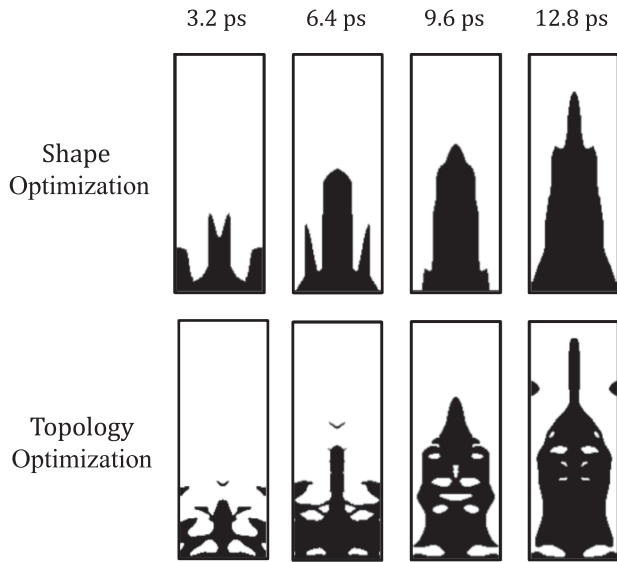
FIG. 6. Shape and topology optimized structures for different group delays (δt = 3.2, 6.4, 9.6, and 12.8 ps).
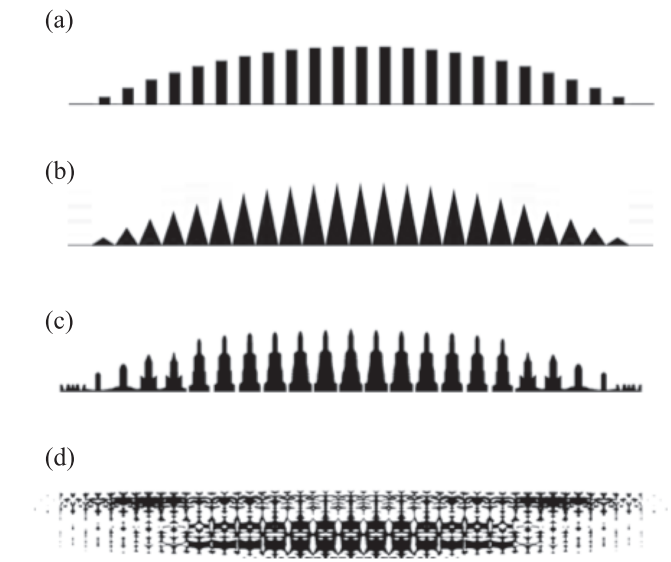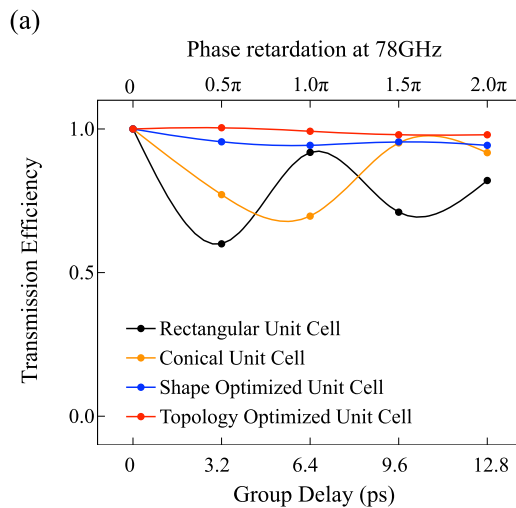

FIG. 8. Metalenses with 70 mm diameter composed of (a) rectangular unit cells, (b) conical unit cells, (c) shape optimized unit cells, and (d) topology optimized unit cells.

We examined the performance of the designed unit cells compared to the conventional rectangular and conical unit cells. To achieve high focusing efficiency, metalens unit cells should have both high transmittance efficiency and small transmittance phase error. Therefore, as the index of the performance, we defined frequency dependent transmittance efficiency $T(\omega)$ and phase error $\delta\theta(\omega)$ of the designed metalens as follows:

$$T(\omega) = |E(\omega)/\tilde{E}_T(\omega)|, \qquad (12)$$

$$\delta\theta(\omega) = arg(E(\omega)) - arg(\tilde{E}_T(\omega)). \qquad (13)$$

The transmittance efficiency [Eq. (12)] is the fraction of transmitted wave through the metalens structure. The phase error [Eq. (13)] is the difference between the phase retardation of the transmitted wave and that of the target wave. When the transmittance efficiency is close to unity and the phase error is close to zero for a broadband frequency range, the metalens unit cell shows superior performance for the broadband frequency range.

In Fig. 5, the transmittance efficiency and the phase error are computed for a rectangular unit cell, conical unit cell, shape optimized unit cell, and topology optimized unit cell. The transmittance
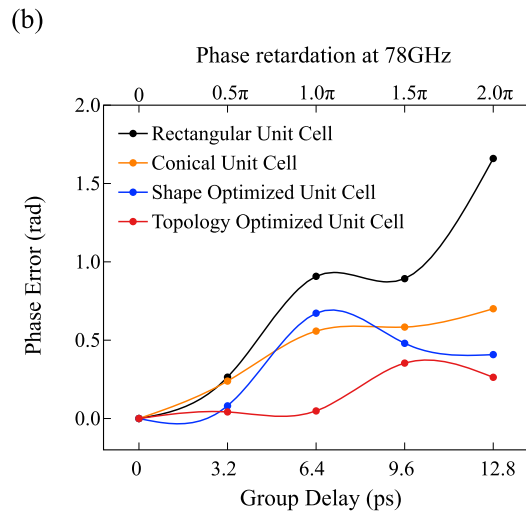

FIG. 7. Averaged transmittance efficiencies and averaged phase errors of rectangular, conical, shape optimized, and topology optimized unit cells for different group delays: (a) transmittance efficiencies and (b) phase errors.
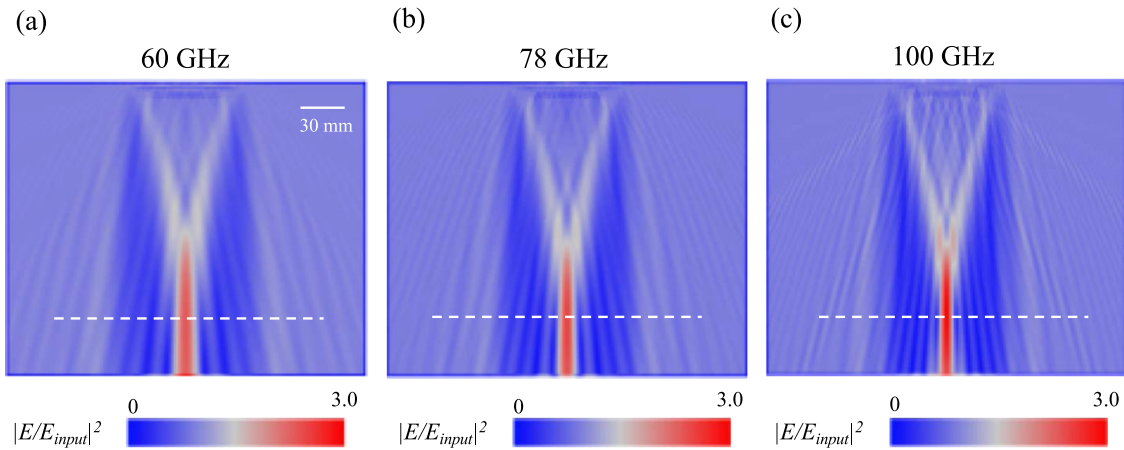
FIG. 9. Electric field intensity distribution of the topology optimized metalens under the illumination of (a) 60 GHz, (b) 78 GHz, and (c) 100 GHz plane waves. The dotted lines show the focal planes.

efficiencies of the conical, shape optimized, and topology optimized unit cells are close to unity. In contrast, the transmittance efficiency of the rectangular unit cell decreases for higher frequency. The transmittance efficiency of the conical unit cell is slightly lower than those of shape optimized and topology optimized unit cells. The phase error is close to zero around the target frequency (78 GHz) for all unit cells, and apart from zero for the surrounding frequency. Apparently, rectangular unit cells have the largest phase error, which will result in relatively narrow band operation. The relative phase errors of conical, shape optimized, and topology optimized unit cells are decreased for broadband frequency. This result demonstrates that unit cells of metalenses with superior

performance were designed by using the proposed topology optimization method.

Next, we provide the shape and topology optimization designs of unit cells that provide different group delays (3.2, 6.4, 9.6, and 12.8 ps) to incident pulses in the time domain. The optimized structures are shown in Fig. 6. The frequency averaged (60–100 GHz) transmittance efficiencies and the absolute value of phase errors are summarized in Fig. 7. It can be seen that for most cases the transmittance efficiencies of the shape and topology optimized unit cells are higher, and the relative phase errors of the optimized unit cells are lower than those of the rectangular and conical unit cells.
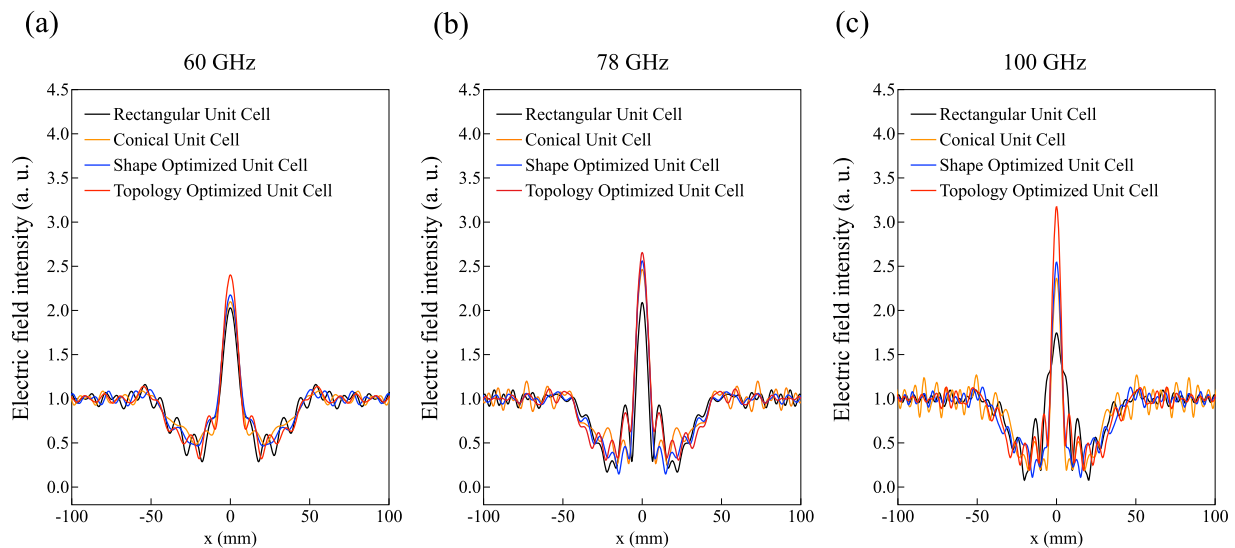

FIG. 10. Electric field intensity along the focal plane for different metalenses under the illumination of (a) 60 GHz, (b) 78 GHz, and (c) 100 GHz plane waves.

Finally, we provide the characteristics of metalenses composed of the optimized unit cells designed by the proposed method. The designed metalenses are shown in Fig. 8. Four metalenses, which are composed of rectangular, conical, shape optimized, and topology optimized unit cells, were designed. We designed metalenses whose focal length is 130 mm with 70 mm diameter. In each design, we arranged 25 unit cells with different retardations calculated by using Eq. (4). The shape and topology optimized unit cells were designed with the same 2D analysis model shown in Fig. 2 other than the absence of the substrate.

Figure 9 shows the electric field intensity distribution of the topology optimized metalens illuminated by 60, 78, and 100 GHz plane waves. It can be observed that the plane waves coming from the top surface were focused into single focal points. Figure 9 demonstrates a small focal length variation of about 100 μm for broadband frequency.

In Fig. 10, the electric field intensity $|E|^2$ along the focal plane is plotted for each metalens. Apparently, a metalens composed of rectangular unit cells shows poor focusing efficiency. Conical, shape optimized, and topology optimized metalenses show similar electric field distributions for the illumination of the 78 GHz wave. However, under the illumination of 60 and 100 GHz waves, the electric field intensity focused by the metalens composed of conical unit cells decreases. We also note that the topology optimized metalens shows the highest electric field intensity for every selected frequency. The result clearly shows that the shape and topology optimized cells attain higher focusing efficiency over broadband frequencies than those of metalenses composed of conventional unit cells, such as rectangular and cone shaped cells.

These results in aggregate demonstrate that the proposed method enables us to design metalens unit cells with superior performance by tuning the structural details.

IV. CONCLUSIONS

In conclusion, we developed a design method of free-form metalens unit cells using time-domain topology optimization and provided the design example of metalens unit cells to operate with enhanced bandwidths at millimeter wavelength. The use of level set functions provided clear optimal structures whose fabrication is practical. We confirm that optimized unit cells of the metalens show superior performance compared to the conventional unit cells for both transmittance efficiency and phase error in broadband wavelength. The proposed method does not depend on the frequency and can be directly applied for different wavelength ranges, such as optical, infrared, and millimeter frequency ranges. Moreover, the proposed time domain optimization method can be applied to not only the design of metalenses, but also the design of other broadband phase modulating flat optical devices, such as metagrating, metacorrector, and diffractive optical elements (DOEs).

DATA AVAILABILITY

The data that support the findings of this study are available from the corresponding author upon reasonable request.

REFERENCES

[1] W. Cai and V. M. Shalaev, *Optical Metamaterials* (Springer, 2010).
[2] A. V. Kildishev, A. Boltasseva, and V. M. Shalaev, Science **339**, 1232009 (2013).
[3] N. Yu and F. Capasso, Nat. Mater. **13**, 139 (2014).
[4] M. Khorasaninejad and F. Capasso, Science **358**, eaam8100 (2017).
[5] W. T. Chen, A. Y. Zhu, and F. Capasso, Nat. Rev. Mater. **5**, 604 (2020).
[6] F. Aieta, P. Genevet, M. A. Kats, N. Yu, R. Blanchard, Z. Gaburro, and F. Capasso, Nano Lett. **12**, 4932 (2012).
[7] F. Aieta, M. A. Kats, P. Genevet, and F. Capasso, Science **347**, 1342 (2015).
[8] P. Lalanne and P. Chavel, Laser Photonics Rev. **11**, 1600295 (2017).
[9] S. Wang, P. C. Wu, V.-C. Su, Y.-C. Lai, C. H. Chu, J.-W. Chen, S.-H. Lu, J. Chen, B. Xu, C.-H. Kuan *et al.*, Nat. Commun. **8**, 187 (2017).
[10] W. T. Chen, A. Y. Zhu, J. Sisler, Z. Bharwani, and F. Capasso, Nat. Commun. **10**, 355 (2019).
[11] W. T. Chen, A. Y. Zhu, V. Sanjeev, M. Khorasaninejad, Z. Shi, E. Lee, and F. Capasso, Nat. Nanotechnol. **13**, 220 (2018).
[12] O. Avayu, E. Almeida, Y. Prior, and T. Ellenbogen, Nat. Commun. **8**, 14992 (2017).
[13] J. S. Jensen and O. Sigmund, Laser Photonics Rev. **5**, 308 (2011).
[14] F. Callewaert, V. Velev, P. Kumar, A. V. Sahakian, and K. Aydin, Sci. Rep. **8**, 1358 (2018).
[15] S. D. Campbell, D. Sell, R. P. Jenkins, E. B. Whiting, J. A. Fan, and D. H. Werner, Opt. Mater. Express **9**, 1842 (2019).
[16] H. Yasuda, T. Yamada, and S. Nishiwaki, Int. J. Numer. Methods Eng. **117**, 605 (2019).
[17] T. Yamada, K. Izui, S. Nishiwaki, and A. Takezawa, Comput. Methods Appl. Mech. Eng. **199**, 2876 (2010).
[18] M. Otomori, T. Yamada, K. Izui, S. Nishiwaki, and J. Andkjær, Comput. Methods Appl. Mech. Eng. **237-240**, 192 (2012).
[19] M. Otomori, T. Yamada, K. Izui, S. Nishiwaki, and N. Kogiso, IEEE Trans. Magn. **50**, 729 (2014).
[20] G. Fujii, H. Watanabe, T. Yamada, T. Ueta, and M. Mizuno, Appl. Phys. Lett. **102**, 251106 (2013).
[21] N. K. Nikolova, H. W. Tam, and M. H. Bakr, IEEE Trans. Microwave Theory Tech. **52**, 1207 (2004).
[22] T. Nomura, K. Sato, K. Taguchi, T. Kashiwa, and S. Nishiwaki, Int. J. Numer. Methods Eng. **71**, 1261 (2007).
[23] Y.-S. Chung, B.-J. Lee, and S.-C. Kim, J. Opt. Soc. Korea **13**, 286 (2009).